International Orthopaedics (2018) 42:1437–1448
https://doi.org/10.1007/s00264-018-3800-7

ORIGINAL PAPER

Application of combined porous tantalum scaffolds loaded with bone morphogenetic protein 7 to repair of osteochondral defect in rabbits*

Qian Wang[1] · Hui Zhang[2] · Hongquan Gan[3] · Hui Wang[4] · Qijia Li[1] · Zhiqiang Wang[3]

Received: 30 August 2017 / Accepted: 23 January 2018 / Published online: 14 February 2018

Abstract

Purpose Porous tantalum (PT) has been widely used in orthopaedic applications for low modulus of elasticity, excellent biocompatibility, and the microstructures similar to cancellous bone. In order to improve the biological activity of PT, biologically active factors can be combined with the material. The purpose of this study was to investigate if bone morphogenetic protein 7 (BMP-7) modifications could enhance the repairing of cartilage of PT in osteochondral defect in medial femoral condyle of rabbits.

Methods A cylindrical osteochondral defect model was created on the animal medial femoral condyle of and filled as follows: PT modified with BMP-7 for MPT group, non-modified PT for the PT group, while no implants were used for the blank group. The regenerated osteochondral tissue was assessed and analyzed by histological observations at four, eight and 16 weeks post-operation and evaluated in an independent and blinded manner by five different observers using a histological score. Osteochondral and subchondral bone defect repair was assessed by micro-CT scan at 16 weeks post-operation, while the biomechanical test was performed at 16 weeks post-operation.

Results Briefly, higher overall histological score was observed in the MPT group compared to PT group. Furthermore, more new osteochondral tissue and bone formed at the interface and inside the inner pores of scaffolds of the MPT group compared to PT group. Additionally, the micro-CT data suggested that the new bone volume fractions and the quantity and quality of trabecular bone, as well as the maximum release force of the bone, were higher in the MPT group compared to PT group.

Conclusions We demonstrated that the applied modified PT with BMP-7 promotes excellent subchondral bone regeneration and may serve as a novel approach for osteochondral defects repair.

Keywords Porous tantalum · Bone morphogenetic protein 7 · Scaffolds · Cartilage engineering · Osteochondral defects

Introduction

Articular cartilage is a tissue of tremendous durability and resilience that permits pain-free movement by greatly reducing friction between bones and distributing stress of numerous loading cycles within our joints. Articular cartilage has a low intrinsic regenerative capacity due to its avascular nature. Unfortunately, when cartilage gets damaged due to injury or disease, it has a limited capacity to heal and can lead to rheumatoid arthritis and joint malfunction.

Regardless of the extensive efforts undertaken to successfully treat and repair cartilage damage and cartilage defects, these still remain very complex issues in clinical practice [1–4]. Although tremendous progress has been made in the field of cartilage repair, current clinical therapies, including hyaluronan injection, subchondral drilling, autologous chondrocyte implantation, and mosaicplasty, still encounter obstacles such as fibrocartilage tissue formation and poor host integration [5–8]. To address these challenges, engineered regenerative medicine has showed a promising role in providing better solutions. Osteochondral autograft transplantation and the mosaicplasty technique are considered a gold standard

Qian Wang and Hui Zhang contributed equally to this work.

✉ Zhiqiang Wang
wzhqde@163.com

[1] Experimental Center, North China University of Science and Technology, Tangshan 063000, China

[2] Department of Joint Surgery 1, The Second Hospital of Tangshan, Tangshan 063000, China

[3] Department of Orthopaedics, Affiliated Hospital, North China University of Science and Technology, No. 73 Jianshe Road, Tangshan 063000, China

[4] Hand Surgery Department, The Second Hospital of Tangshan, Tangshan 063000, China

Table 1 Material physical and chemical performance indicators

Indicators	Range
Density (g/cm^3)	3.5–7
Porosity (%)	65–80
Pore diameter (μm)	400–600
Elasticity modulus (GPa)	2.0–4.6
Ultimate strength (MPa)	110–210
Yield strength (MPa)	75–120
Compressive strength (MPa)	100–170
Tensile strength (MPa)	80–120
Bending strength (MPa)	80–150

among the grafts. However, these methods are plagued by limited donor sources, site morbidity, pain, and the risk of infection as well as poor integration between the host and donor tissues. The ideal orthopaedic implant material should have good biocompatibility, enough mechanical strength, three-dimensional porous structures similar to normal bone, good plasticity, osteoconduction, and osteoinduction. Recently, trabecular metal (TM) has been used in revision arthroplasty procedures and for variety of different applications in reconstructive orthopaedic surgery [9–13]. TM has a high mechanical strength that can provide good support for new tissue growth, which is especially suitable for load-bearing parts of bone repair. The commonly used porous metal materials are porous tantalum (PT), porous titanium, and their alloys. The porous structure can facilitate the ingrowth of bone tissue and form anchorage, significantly enhancing the bonding strength between bone and implant. The rough surface can effectively improve the stability of PT implant in vivo. Furthermore, the porosity of PT material is 75~85%, with average pore diameter of 400~600 μm, which is very suitable for the entry of cells [14–17]. However, the widespread use of PT in China is limited by the high price. To solve this problem, in cooperation with numerous domestic research institutions, Chongqing Runze Pharmaceutical Co., Ltd. (Chongqing, China) has successfully developed PT materials, prepared by slip-casting powder through teeming technology. The physical and mechanical indexes showed that this kind of PT possesses high porosity (65–80%), appropriate pore diameter size (400–600 μm), and good mechanical characteristics (Table 1) similar to those of human bone. The PT may serve as an excellent substitute material for bone graft in the future.

Nevertheless, tantalum is a kind of inert metal material, and lack of adequate tissue-implant integration can lead to early implant failure, which is actually one of the most significant clinical challenges. Strategies attempting to address this issue include generating porous implant surfaces to encourage bone ingrowth, applying biological interface for adhesion proliferation and differentiation of seed cells, promoting the generation and calcification of extracellular matrix to establish solid bone interface, and meeting the requirements of clinical early weight-bearing activities. In a previous study, we found that PT scaffolds modified with the RGD peptide can enhance repair of segmental bone defects in rabbit radius [18]. This time, we used bone morphogenetic protein 7 (BMP-7) for surface modification, which has been used in bone and cartilage repair [19–21]. BMP-7 plays an important role in bone development, bone defect repair, and cartilage differentiation and is commonly associated with fibronectin and accelerates cartilage defect healing [22–25]. In our previous experiment, BMP-7 had shown the good bioability in promoting chondrocyte adhesion and proliferation on the surface of PT in vitro.

The purpose of this study was to investigate if BMP-7 modifications could enhance the repairing of cartilage of PT in osteochondral defect in medial femoral condyle of rabbits and to provide experimental evidence for future clinical applications.

Materials and methods

Animals

Forty-eight adult male New Zealand white rabbits (weight, 2.5–3.0 kg) were provided by the Experimental Animal Center of North China University of Science and Technology (Tangshan, China). All animal studies (including the mice euthanasia procedure and experimental protocols) were done in compliance with the regulations and guidelines

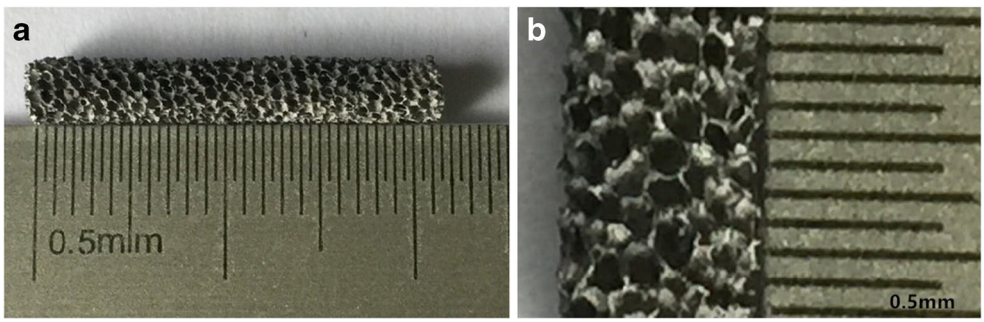

Fig. 1 Appearance of porous tantalum

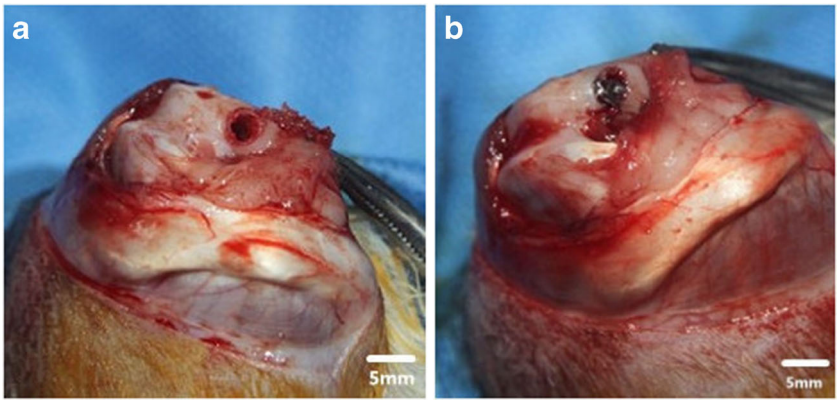

Fig. 2 The operation process. **a** Osteochondral defect on the condylus medialis femoris (right). **b** Porous tantalum was implanted into the defect on the medial femoral

of North China University of Science and Technology Institutional Animal Care and conducted according to the AAALAC and the IACUC guidelines.

Biomaterial preparation

PT (Chongqing Runze Pharmaceutical Co., Ltd.) selected was − 250-mesh pure tantalum powder with a certain amount of additives and added sponge carrier to control the pore diameter of porous materials, porosity, and pore distribution and approved by slip-casting forming and through 1500–2100-°C high temperature sintered and post-treatment technology of necessary preparation (preparation method has been submitted for patenting). The PT scaffolds were oval-shaped cylinders, 4 mm in diameter and 5 mm in height (Fig. 1). All sample rods were rinsed with double distilled water, autoclaved, and exposed to UV light for 20 min prior each experiment.

Tantalum loaded with BMP-7 (ProSpec company, pro-770, Israel) was prepared according the following protocol: 5-mg rhBMP-7 was dissolved at a concentration of 10 ml of 6-M urea solution. Consequently, PT rods were immersed in the solution, preserved for 12 hours in 4 °C, and then freeze-dried and disinfected with chloroform steam.

Surgical procedure

Forty-eight rabbits were randomly divided into three groups: all rabbits were operated, modified porous tantalum (MPT) group ($n = 20$), PT group ($n = 20$), and blank group ($n = 8$) (two extra rabbits in each group to ensure sufficient sample size). The materials were implanted on the right side of the medial femoral condyle. Surgical procedures were performed under general anesthesia (intraperitoneal injection of 10% chloral hydrate). Briefly, after preforming the medial parapatellar arthrotomy, the patella was dislocated and flipped laterally. A 4-mm-diameter, 5 mm-deep osteochondral defect was then created in the femoral medial condyle using a dental drill. The defects were carefully and sufficiently lavaged using 0.9% saline solution. Rods were then inserted into the right knee hole in the MPT and PT groups (Fig. 2). Contrary, osteochondral defects in the knee treated with matrix were used for a blank group. Consequently, rabbits were allowed unrestricted motion within their cages and operated limbs were not immobilized. After four, eight and 16 weeks post-operation, rabbits were euthanized and the treated knees were harvested and analyzed in ex vivo. Post-operative animal care was done by experienced trained personnel and supervised by veterinarians.

General observations

Bone defect sites and bone surrounding areas were harvested on four, eight and 16 weeks post-operation. The cartilage defects were observed to examine bone defect healing. Boner repair effect of each group was analyzed according the general standard [26, 27] (Table 2).

Table 2 Gross observation standard for evaluation of cartilage defect repair

Observation index	Score
Repair defective edge	
Completely covered defect area	2
Partially covered defect area	1
Uncovered defect area	0
Surface regularity smooth and intact	
Smooth and intact	2
Partially smooth and intact	1
Rough	0
The defect filled	
Completely filled defect area	2
Partially filled defect area and slight depression	1
Significant depression or overgrowth	0
Neocartilage color and transparency	
Transparent	2
Translucent	1
Opaque	0

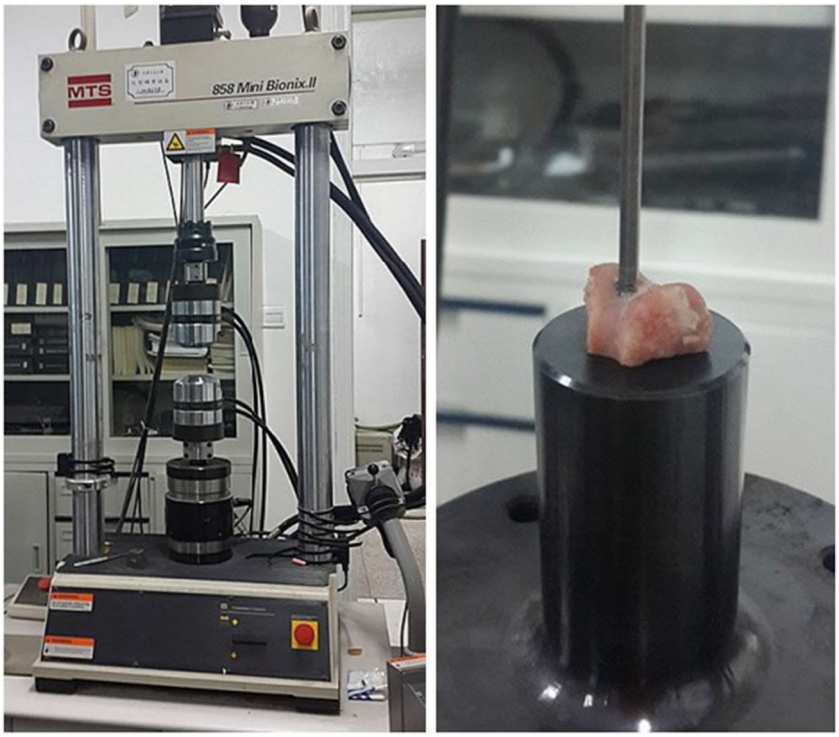

Fig. 3 The images of MTS- 858 and push-out testing

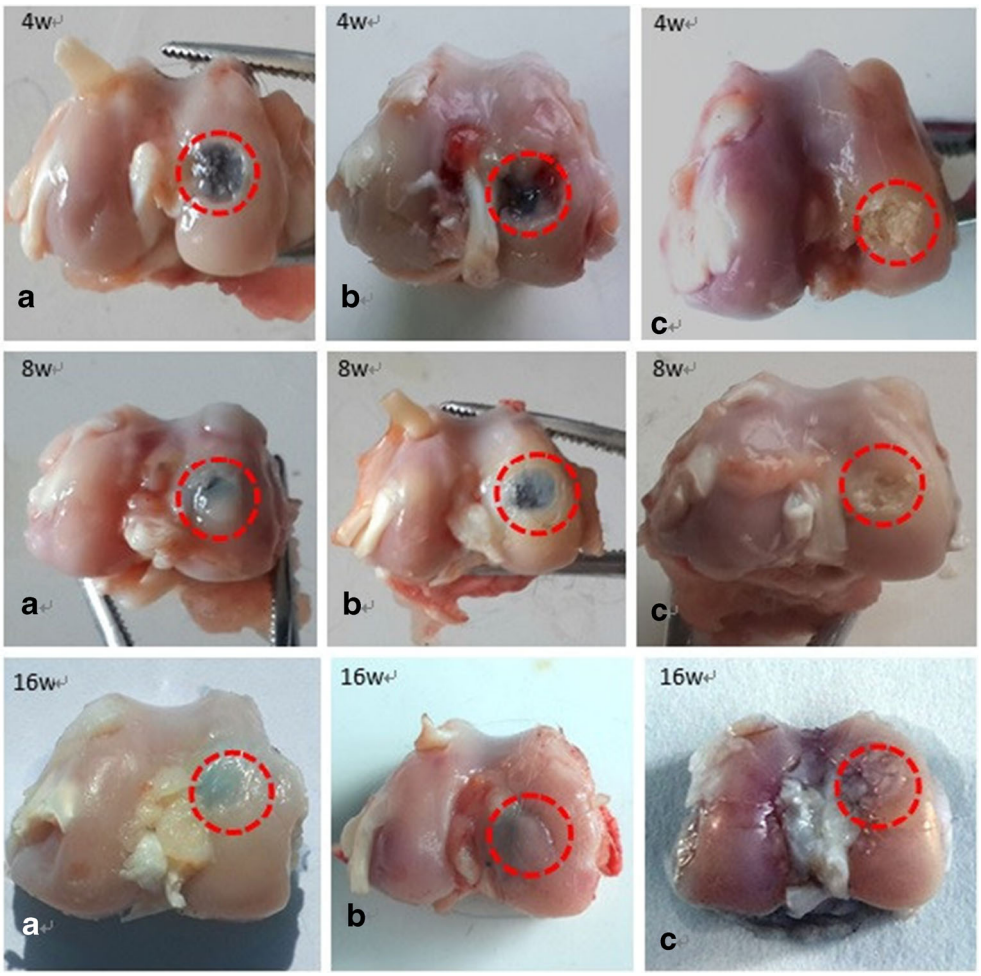

Fig. 4 Gross appearances during 4, 8, and 16 weeks in **a** MPT group, **b** PT group, and **c** blank group

Scanning electron microscope analysis

The PTs were removed and analyzed on four, eight and 16 weeks post-operation, and histological evaluations were sequentially performed on the same specimen. Briefly, the specimen was washed twice using 0.1% phosphate buffer, dehydrated with gradient tert-butanol, and stored at − 10 °C for one hour. Consequently, the specimen was dried using vacuum, fixed using conductive adhesive on the copper, and metal spraying. Finally, the tantalum rod surface of cartilage and bone tissue growth was observed by SEM.

Hard tissue section analysis

After observing the experimental animal specimens, the implant material with surrounding 0.5-cm tissue was removed, washed with PBS, then trimmed, and fixed in 10% formaldehyde. Following dehydration, infiltration, embedding (20-g benzoyl peroxide in 800-ml methacrylic acid methyl ester, phthalic acid, and 200-ml dibutyl), and polymerization, a metal slicer was used to cut the material along the direction parallel to the longitudinal axis of the PT rod, fully exposing its plane. The plane was polished and 70-μm slices were prepared, which were ground down to 20 μm, dried, and exposed to glycol ether ester to remove any plastic. The optical microscope was used to observe the tissue voids within the cartilage, as well as the growth of the bone within the PT and surroundings.

CT examination

On 16 weeks post-operation, three specimens were randomly selected from MPT and PT groups, respectively, and the PT and the surrounding bone were scanned using an micro-CT device (eXplore Locus SP, GE Healthcare, London, Canada). Three specimens of each groups around the bubble fixed were placed vertically in the sample holder. The scanning parameters were as follows: 14-μm resolution, 270-minute scanning time, 360° rotation, 0.4° rotation angle increment, 3000-ms exposure time, 80 kV, 80 μA, 2960-ms exposure time, the average frame of 4, and pixel combination for 1 × 1. The interface and the surrounding bone in 16 weeks were observed and analyzed using three-dimensional reconstruction, reconstruction fringe normalization correction software, Hounsfield scale correction, and visualization software (MicroView ABA 2.1.2, GE Healthcare, London, Canada).

PT material and the surrounding area of the 5-mm diameter cylindrical were selected as main region of interest (RIO). Main parameters of the software automatic generation included: (1) bone intertrabecular space (trabecular spacing, Tb. Sp), μm representation; (2) bone density of tissue mineral density (tissue mineral density, TMD): per unit volume is higher than the set value of bone mass, expressed in mg/cm^3; (3) bone trabecular thickness (trabecular thickness, Tb, Th); (4) trabecular number (trabecular number, Tb. N), expressed as a 1 mm; and (5) bone volume fraction (bone volume fraction, BV/TV) which the trabecular bone volume (BV) divided by the ROI volume (TV), expressed as %.

Table 3 The gross score of cartilage repair ($\overline{X} \pm S$, $n = 6$)

Group	4w	8w	16w
A	2.500 ± 0.548	5.500 ± 0.548*	7.833 ± 0.408*
B	2.167 ± 0.408	4.000 ± 0.632	5.167 ± 0.753
t value	1.195	4.392	7.628
P value	0.260	0.001	0.000

*Compare with B group, $P < 0.05$

Launch experimental

In this study, the displacements recorded by MTS 858 (MTS Inc., Arlington, VA, USA) were used to calculate the specimen deformation. Briefly, on the 16 weeks post-operation, six specimens were randomly selected from MPT and PT groups, respectively. The specimen sections were placed on the MTS device, and the launch test was performed using the displacement rate of 2 mm/min until the specimen loosed. Consequently, stress/displacement curve, stress plot, and deformation were measured [28] (Fig. 3).

Statistical analysis

Values were presented as mean ± standard error of mean (SEM). ANOVA and Student's *t* test were used to compare data between groups. $P < 0.05$ was considered as significant different. Data collected from quantitative parameter was analyzed using independent *t* test. Values were presented as mean ± SEM. Differences at 5% level were considered significant. All analyses were performed using SPSS 20.0 software.

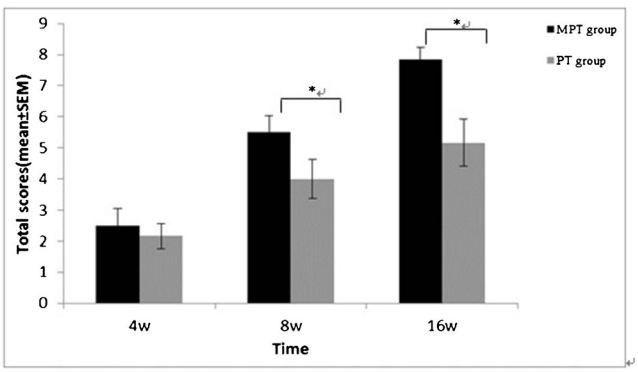

Fig. 5 The gross score of cartilage repair

Results

Post-operative observations

All rabbits were awake within 2 h after the operation and were immediately placed on a normal diet. Movement and body weight two weeks post-operatively. No post-operative complications such as wound dehiscence or infections were observed. All the animals survived uneventfully.

General observation

In week four, small amount of cartilage like-tissue was observed on the defect surface of MPT group, while no tissue was observed in the PT group (Fig. 4, fourth week). Consequently, in week eight, cartilage like-tissue was observed in both MPT and PT groups (Fig. 4, eighth week). Moreover, defects in the untreated rabbits (blank group) did not heal (Fig. 4c). In addition, incomplete osseous filling with a purely fibrous top layer was found in the blank group. Moreover, no signs of tissue inflammation and graft-host reaction were observed in MPT and PT groups. Histological score suggested that the cartilage repair gross score was spastically higher ($P < 0.05$) in eight and 16 weeks post-operation in the MPT group compared to a PT group (Table 3) (Fig. 5).

Microscopic analyses of porous tantalum

Surface characteristics of PT discs were observed under SEM, (Fig. 6). Briefly, open three-dimensional structures of Ta with dodecahedral pores fully interconnected by smaller openings were observed. Material surface and cross-sections had an interconnected pore distribution, with a pore diameter of 400–600 μm. The trabecular pillars had a microporous structure, with a diameter of 100 μm. Pore distribution was uniform and the pores were interconnected.

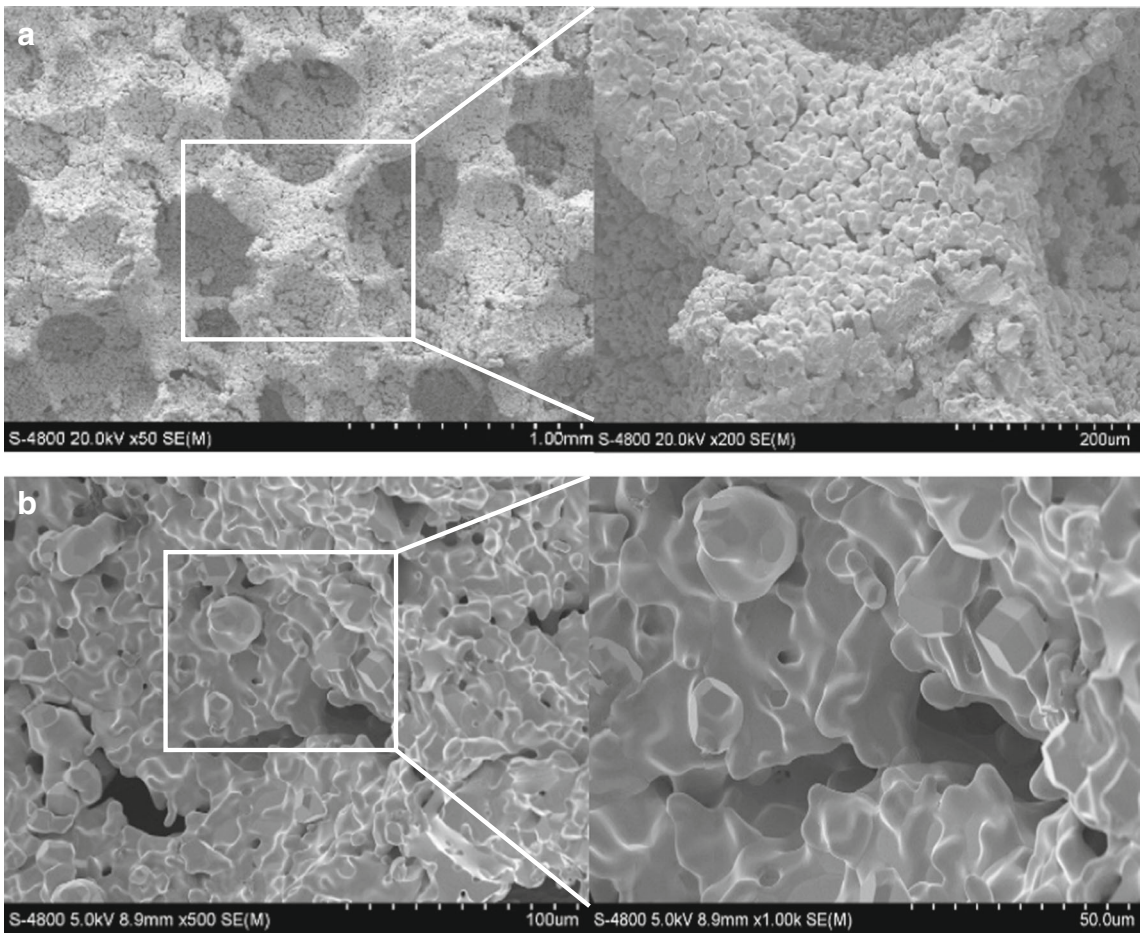

Fig. 6 Scanning electron micrographs of unseeded porous tantalum using 50, 200, 500, and 1000 magnification. **a** Porous tantalum specimen morphology, with a rough and irregular surface and interconnected pores with diameters of 400–600 μm. Material surface and cross-section show interconnected pore distribution, with a pore diameter size of 200–400 μm (scale bar, 200 μm). **b** Trabecular pillar exhibits a micropore structure, with the diameter of the interval of the trabecular pillar 100 μm (scale bar, 100 μm). Micropore structure of the trabecular pillar, where the diameter of the micropores was 10 μm (scale bar, 50 μm)

The microporous structure with interconnected pores had a diameter of 200–400 μm, the particle diameter was 20–50 μm, and there were 50–200-μm interstices between the particles (Fig. 6a–e).

Microscopic analyses of the implant and the surrounding tissue

Four weeks post-operation, small amounts of calcium salt, new cartilage, and osteoblasts were found on the material surface in MPT and PT group. Osteoblasts were attached to PT surface by pseudopodia. Small amount of new bone tissue was observed within the pores in both groups. Most importantly, during week four, higher amount of calcium salt deposition, higher cartilage formation, and higher number of osteoblast were observed in the MPT group compared to PT. Consequently, during weeks eight and 16, the deposition of calcium salt gradually increased, the new cartilage and bone cells connected the flakes, extracellular matrix covered the surface pores of PT, and the emergence of a large number of new bone tissue was observed, in both groups; however, once aging, higher amount of calcium salt deposition and extracellular matrix coverage were observed in the MPT group compared to PT (Fig. 7).

Histological analyses

At four, eight and 16 weeks after surgery, new bone mass and maturity gradually increased at the interface and inside the inner pores in the MPT and PT groups, the new bone gradually grew from the surrounding to the inner pore, and the new bone formed in the MPT group was better than that of the PT group (Fig. 8).

Micro-CT analysis

Cross-sectional and coronal scanning as well as three-dimensional reconstruction images at 16 weeks after surgery showed that there were newly formed bones in the surrounding and inner pores of the implants; the combination at the interface between the implant and host bone was firm without PT fracture (Fig. 9). On the 16th week after surgery, every specimen scanning results of three-dimensional reconstruction and bone histomorphometric analysis showed that the interior surface and the surrounding bone TMD, BV/TV, TB. N, as well as the TB. Th, and Tb. Sp were significantly higher in the MPT compared to the PT group ($P < 0.05$), however the Tb. Sp (Table 4).

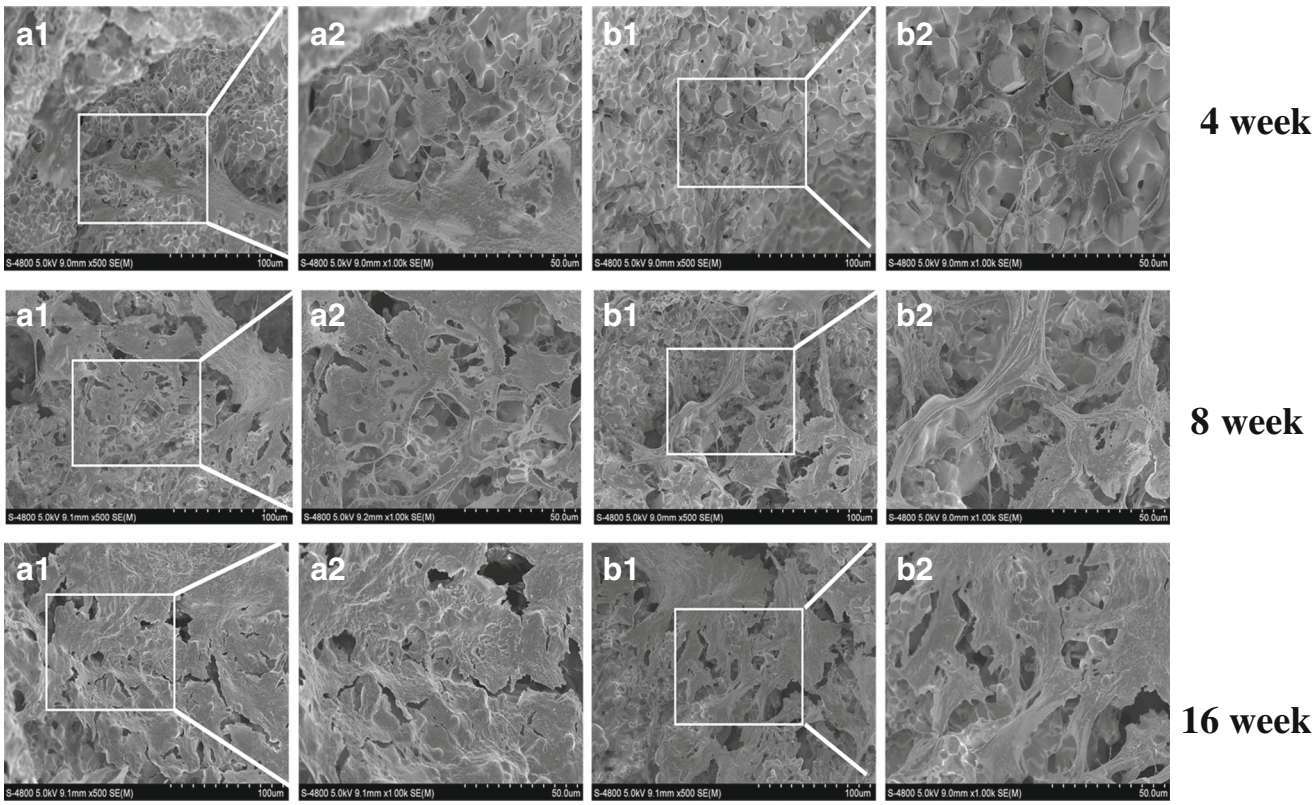

Fig. 7 The SEM images of porous tantalum after surgery (SEM ×1000) in **a** MPT group and **b** PT group. 1: 4 weeks; 2: 8 weeks; 3: 16 weeks

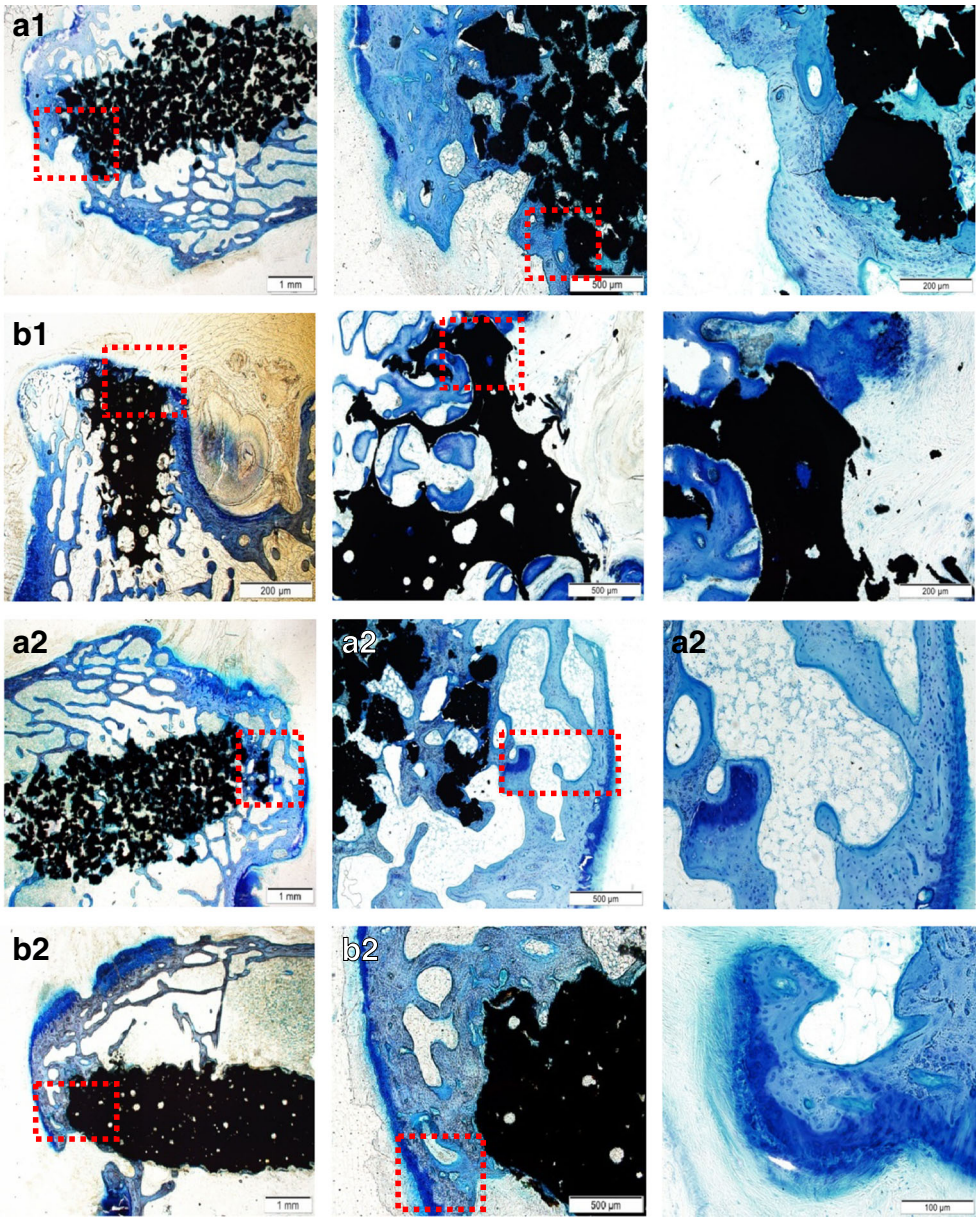

Fig. 8 The toluidine-blue-stain of repaired osteochondral defects after surgery in **a** MPT group, **b** PT group. 1: 4 weeks; 2: 8 weeks; 3: 16 weeks

Launch experimental analysis

During four, eight and 16 weeks after surgery, the launch experimental results showed that the maximum launch force increased overtime in both groups. However, the higher maximum launch force was observed in the MPT group compared to PT group ($P < 0.01$) (Table 5).

Discussion

Injuries of cartilage and subchondral bone are still challenging issues in orthopaedics. Bone graft replacement is one of the commonly employed methods for the treatment of cartilage defects. Suitable bone graft materials should possess the spatial structure, mechanical properties, and bone induction. At the same time, with cartilage subchondral bone being damaged, the material should provide good support for subchondral bone defect and a good platform for the repair of articular cartilage injury. Thus far, PT has shown to be a promising material for bone tissue engineering. The PT has high porosity (75–80%), good tissue compatibility, a large surface friction coefficient, and the appropriate elastic modulus that closely matches that of human bone. Due to all these qualities, PT has been widely applied in arthroplasty, spinal fusion surgery, and the femoral head necrosis treatment [29, 30]. BMP-7 is a member of the bone morphogenetic protein family, which has very strong ectopic osteogenesis, can form ectopic new bone, and has an important role in the repair of bone defects and cartilage differentiation [31, 32]. Engineered

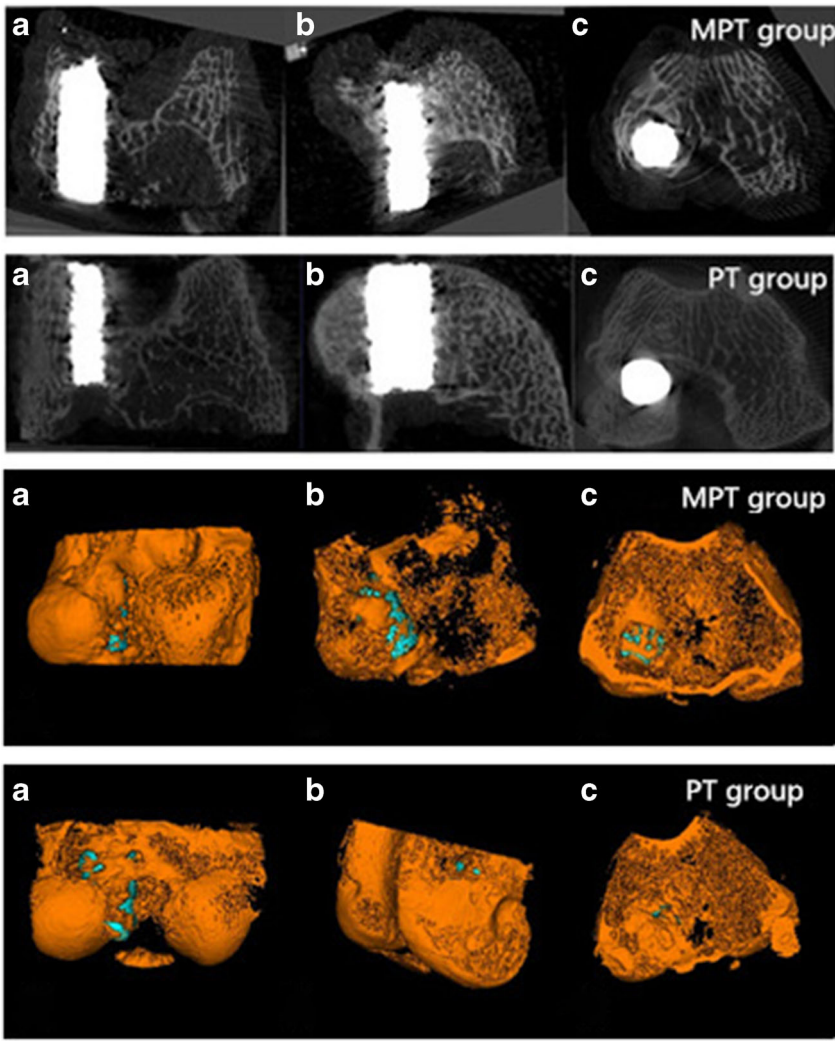

Fig. 9 Coronal (**a**), sagittal (**b**), and transverse (**c**) images of and 3D reconstructed micro-CT in each group at 16 weeks after the operation

regenerative medicine and supplemental growth factors have been used to repair damaged hyaline cartilage; nevertheless, there are only few reports relating to the development in recipient's defective region from scaffold implantation during the post-operative rehabilitation stage [33–36]. In the present study, the PT material was loaded with BMP-7 and was implanted in the rabbit model with femoral condyle cartilage defect. Gross observation, hard tissue section, SEM method, micro-CT, and biomechanical experiments were used to observe the effect of PT and BMP-7 complex on rabbit articular subchondral bone and cartilage defect repair and to provide experimental evidence for future clinical applications. The limitation of the present study is a lack of BMP-7 only group, which would provide more information about the BMP-7 promoting repairing process of osteochondral defect. A previous study used fibrin gel combined with porous titanium as scaffold material, to investigate the effects of BMP-2 on bone defect repairing, with a BMP-2 only group that loaded BMP-2 on fibrin gel only [37]. However, in the present study, we used the PT as the only scaffold material in the present

Table 4 The results of bone histomorphometry ($\overline{X} \pm S$, $n = 6$)

	MPT group	PT group	T	P
TMD (mg/cm^3)	992.608 ± 10.845*	856.523 ± 16.435	16.929	0.000
BV/TV (%)	0.193 ± 0.007*	0.122 ± 0.008	16.882	0.000
Tb. N (mm)	41.643 ± 1.185*	33.69 ± 1.153	10.066	0.000
Tb. Th (mm-1)	3.793 ± 0.053*	3.298 ± 0.098	10.919	0.000
Tb. Sp (mm)	192.967 ± 11.799*	271.925 ± 9.803	12.608	0.000

*Compare with PT group, $P < 0.05$

Table 5 The maximum release force (unit: Newton, $\overline{X} \pm S$, $n = 6$)

Group	4w	8w	16w	F	P
MPT	291.764 ± 16.599*	506.332 ± 21.348*a	620.775 ± 23.211*ab	395.39	0
PT	230.511 ± 20.221	434.730 ± 16.236	515.125 ± 20.205	358.57	0
T	5.74	6.54	8.41		
P	0	0	0		

*Compare with PT group, $P < 0.05$

study, which limited our ability to set up an only BMP-7 group. Further, we do not think it is appropriate that injection of BMP-7 is only in the osteochondral defect without any scaffold material.

In the present study, we established rabbit model with femoral condyle cartilage defect in the femoral condyle weight-bearing area which is the predilection site.

Previous studies have suggested that after six weeks, the defect diameter less than 3 mm will partly or completely heal; so in the present study, we selected the defect region with 4-mm diameter and 5-mm depth [38]. Experimental results revealed that in the control group, 16 weeks post-surgery, cartilage defect regions were covered with fibrous tissue and fibrocartilage, and there was no self-healing. Also PT compound BMP-7 group and pure PT group had different levels of repair, which implies that the models were successful.

Post-operative general observations that increased with time were as follows: the combined material and host bone gradually closed, cartilage defect region was gradually covered by new cartilage tissue, and the overall situation of the cartilage repair with PT compound BMP-7 was better compared to PT group. The control group also observed a successful healing, but with the internal defect formation and without the formation of chondroid tissue. The results suggested that PT could repair the defect of the subchondral bone; nevertheless, the high pore ratio and porosity of the composite materials are beneficial for the osmotic release of BMP-7 and the transfer of cellular factors from the host bone to the defected regions, which in turn provides favorable conditions for cartilage repair. Previous studies have shown that BMP-7 compound with biological materials can significantly accelerate the integration of host bone and material and has the obvious effect on bone conduction [39]. The results of this study also suggest that the PT compound with BMP-7 can create the microenvironment favourable for cartilage and bone regeneration and provide a new experimental basis for repairing cartilage defect.

In the present study, hard-tissue specimen sections were observed after implantation and the implanted tantalum rods were taken out and scanned with electron microscope. Results showed that with time, new cartilage and bone cells appeared and increased on the interface of PT and host bone; the new formed bone trabeculae began to grow into the pores; bone tissue gradually combined with PT; and cartilage defect areas were gradually covered by chondroid-like tissues. Hard tissue slices and scanning electron microscopy results showed that PT compound with BMP-7 was better compared to PT. From the previous research on PT acetabular implantation in dogs, the histology and SEM results of the combination of bone and prosthesis interface found that the bone ingrowth depth was 0.2–1.2 mm, meaning host bone and prosthesis can form a solid combination [40]. These conclusions were very similar to ours. Furthermore, 16 weeks post-operatively, the specimens were scanned by micro-CT for three-dimensional reconstructions and measured by bone histomorphometry. There was a small amount of trabecular bone around the material which gradually increased and finally achieved good integration with the surrounding host bone. Nevertheless, the quantity and thickness of trabecular bone of PT were significantly lower compared to the PT compound with BMP-7 group.

In the previous study of porous titanium composite/type I collagen scaffold used to repair cartilage defect in canine model in glycosaminoglycan, micro-CT results showed that the new bone tissue around the scaffold was higher compared to scaffold itself, which overall had good healing effect on the cartilage defected area, and the results were similar to ours [41]. There are studies found that cartilage-associated genes (collagen type II, AggC, Sox 9) could affect growth of cartilage tissue [42]. And some researchers have put forward and defined the term chondroconductive as providing a scaffold for the growth of cartilage and supporting structures [43]. PT has an open-pore structure; it seems to stimulate the growth of cartilage. They predicted that the remaining defect will then be filled by periosteum-derived subchondral bone and neocartilage formation. The strong bone integration capacity of TM and the high grade of integration are observed from periosteal chondrogenesis. In this study, PT combined with BMP-7 may also promote hyaline-like cartilage tissue by affecting cartilage-associated genes and established the support of the subchondral bone to complete the development of periosteal cartilage. However, the concrete mechanism will still remain pending further investigation.

Furthermore, the biomechanical test was performed on the samples, revealing that with the increase of time, the maximum power of every group gradually increased, and the time data point were statistically different. At each time point, the maximum power of the PT composite BMP-7 group was greater compared to the PT group, and the difference was

statistically significant ($P < 0.05$). Also, the maximum power of the PT composite BMP-7 group was greater compared to the PT group ($P < 0.05$). These results suggest that PT can form good integration with the host bone, and the better composite effect is achieved with addition of BMP-7. The rough surface of PT can enlarge the contact area with the host bone and porous structure can form the mechanical interaction necessary for bone ingrowth [44, 45].

According to the experimental results and presented research review, PT compound with BMP-7 can form stable connection and integration with the host, promoting cartilage and subchondral bone defect healing. Furthermore, it provides a new experimental basis for further cartilage and bone injury repair via tissue engineering scaffolds.

Acknowledgements We thank Dr. Jun Wang from Xijing Hosipital affiliated, Fourth Military Medical University of China for technical help in micro-CT.

Funding information This study was funded by the National Key Technology Support Program of China (Contract Grant No. 2012BAE06B03).

Compliance with ethical standards

Ethical approval All procedures performed in this study involving animals were in accordance with the ethical standards of the institution at which the study was conducted.

Conflict of interest The authors declare that they have no conflict of interest.

References

1. Bouwmeester SJ, Beckers JM, Kuijer R, Linden AJ, Bulstra SK (1997) Long-term results of rib perichondrial grafts for repair of cartilage defects in the human knee. Int Orthop 21(5):313–317
2. Gillogly SD (2003) Treatment of large full-thickness chondral defects of the knee with autologous chondrocyte implantation. Arthroscopy 19(Suppl 1):147–153
3. Marcacci M, Kon E, Zaffagnini S, Vascellari A, Neri MP, Iacono F (2003) New cell-based technologies in bone and cartilage tissue engineering. I. Bone reconstruction. Chir Organi Mov 88(1):33–42
4. Henderson I, Tuy B, Oakes B (2004) Reoperation after autologous chondrocyte implantation. Indications and findings. J Bone Joint Surg Br 86(2):205–211
5. Marin E, Fedrizzi L, Zagra L (2010) Porous metallic structures for orthopaedic applications: a short review of materials and technologies. Eur Orthop Traumatol 1(3–4):103–109
6. Helm AT, Kerin C, Ghalayini SRA, Mclauchlan GJ (2009) Preliminary results of an uncemented trabecular metal tibial component in total knee arthroplasty. J Arthroplast 24(6):941–944
7. Cardaropoli F, Alfieri V, Caiazzo F, Sergi V (2012) Manufacturing of porous biomaterials for dental implant applications through selective laser melting. Adv Mater Res 535-537(3):1222–1229
8. Bobyn JD, Poggie RA, Krygier JJ, Lewallen DG, Hanssen AD, Lewis RJ, Unger AS, O'Keefe TJ, Christie MJ, Nasser S, Wood JE, Stulberg SD, Tanzer M (2004) Clinical validation of a structural porous tantalum biomaterial for adult reconstruction. J Bone Joint Surg 86-A Suppl 2(suppl 2):123–129
9. Matsuno H, Yokoyama A, Watari F, Uo M, Kawasaki T (2001) Biocompatibility and osteogenesis of refractory metal implants, titanium, hafnium, niobium, tantalum and rhenium. Biomaterials 22(11):1253–1262
10. Bobyn JD, Stackpool GH, Hacking SA, Tanzer M, Krygier JJ (1999) Characteristics of bone ingrowth and interface mechanics of a new porous tantalum biomaterial. J Bone Joint Surg Br 81(5):907–914
11. Findlay DM, Welldon K, Atkins GJ, Howie DW, Zannettino AC, Bobyn D (2004) The proliferation and phenotypic expression of human osteoblasts on tantalum metal. Biomaterials 25(12):2215–2227
12. Johansson CB, Hansson HA, Albrektsson T (1990) Qualitative interfacial study between bone and tantalum, niobium or commercially pure titanium. Biomaterials 11(4):277–280
13. Zhang M, Wang GL, Zhang HF, Hu XD, Shi XY, Li S, Lin W (2014) Repair of segmental long bone defect in a rabbit radius nonunion model: comparison of cylindrical porous titanium and hydroxyapatite scaffolds. Artif Organs 38(6):493–502
14. Periasamy K, Watson WS, Mohammed A, Murray H, Walker B, Patil S, Meek RM (2011) A randomised study of peri-prosthetic bone density after cemented versus trabecular fixation of a polyethylene acetabular component. J Bone Joint Surg Br 93(8):1033–1044
15. Harrison AK, Gioe TJ, Simonelli C, Tatman PJ, Schoeller MC (2010) Do porous tantalum implants help preserve bone: evaluation of tibial bone density surrounding tantalum tibial implants in TKA. Clin Orthop Relat Res 468(10):2739–2745
16. Amanatullah DF, Farac R, McDonald TJ, Moehring HD, Cesare PED (2013) Subtrochanteric Fracture following removal of a porous tantalum implant. Case Rep Orthop: 946745
17. Sinclair SK, Konz GJ, Dawson JM, Epperson RT, Bloebaum RD (2012) Host bone response to polyetheretherketone versus porous tantalum implants for cervical spinal fusion in a goat model. Spine 37(10):E571–E580
18. Wang H, Li Q, Wang Q, Shi W, Gan H, Song H, Wang Z (2017) Enhanced repair of segmental bone defects in rabbit radius by porous tantalum scaffolds modified with the RGD peptide. J Mater Sci Mater Med 28(3):50
19. Sakou T (1998) Bone morphogenetic proteins: from basic studies to clinical approaches. Bone 22(6):591–603
20. Chubinskaya S, Merrihew C, Cs-Szabo G, Mollenhauer J, McCartney J, Rueger DC, Kuettner KE (2000) Human articular chondrocytes express osteogenic protein-1. J Histochem Cytochem 48(2):239–250
21. Mori H, Kondo E, Kawaguchi Y, Kitamura N, Nagai N, Iida H, Yasuda K (2013) Development of a salmon-derived crosslinked atelocollagen sponge disc containing osteogenicprotein-1 for articular cartilage regeneration: in vivo evaluations with rabbits. BMC Musculoskelet Disord 14(1):174
22. Chubinskaya S, Kawakami M, Rappoport L, Matsumoto T, Migita N, Rueger DC (2007) Anti-catabolic effect of OP-1 in chronically compressed intervertebral discs. J Ortho Res 25(4):517–530
23. Mason JM, Grande DA, Barcia M, Grant R, Pergolizzi RG, Breitbart AS (1998) Expression of human bone morphogenic protein 7 in primary rabbit periosteal cells: potential utility in gene therapy for osteochondral repair. Gene Ther 5(8):1098–1104
24. Mason JM, Breitbart AS, Barcia M, Porti D, Pergolizzi RG, Grande DA (2000) Cartilage and bone regeneration using gene enhanced tissue engineering. Clin Orthop Relat Res 379(379 Suppl):S171–S178
25. Vinall RL, Lo SH, Reddi AH (2002) Regulation of articular chondrocyte phenotype by bone morphogenetic protein-7, Interleukin-1, and cellular context is dependent on the cytoskeleton. Exp Cell Res 272(1):32–44
26. Moran ME, Kim HK, Salter RB (1992) Biological resurfacing of full-thickness defects in patellar articular cartilage of the rabbit.

Investigation of autogenous periosteal grafts subjected to continuous passive motion. J Bone Joint Surg Br 74(5):659–667
27. Niederauer GG, Slivka MA, Leatherbury NC, Korvick DL, Harroff HH, Ehler WC, Dunn CJ, Kieswetter K (2000) Evaluation of multiphase implants for repair of focal osteochondral defects in goats. Biomaterials 21(24):2561–2574
28. Duan K, Hu YX, Long K, Toms A, Burt HM, Oxland TR, Masri BA, Duncan CP, Garbuz DS, Wang R (2012) Effect of alendronate-containing coatings on osteointergration into porous tantalum in a cortical bone model. Nano Life 2 (01):l-12
29. Wang JC, Yu WD, Sandhu HS, Tam V, Delamarter RB (1998) A comparison of magnetic resonance and computed tomographicimage quality after the implantation of tantalum and titanium spinal instrumentation. Spine 23(15):1684–1688
30. Zardiackas LD, Parsell DE, Dillon LD, Mitchell DW, Nunnery LA, Poggie R (2001) Structure, metallurgy, and mechanical properties of a porous tantalum foam. J Biomed Mater Res 58(2):180–187
31. Papanna MC, Al-Hadithy N, Somanchi BV, Sewell MD, Robinson PM, Khan SA, Wilkes RA (2012) The use of bone morphogenic protein-7 (OP-1) in the management of resistant non-unions in the upper and lower limb. Injury 43(7):1135–1140
32. Zamurovic N, Cappellen D, Rohner D, Susa M (2004) Coordinated activation of notch, Wnt, and transforming growth factor-beta signaling pathways in bone morphogenic protein 2-induced osteogenesis. Notch target gene Hey1 inhibits mineralization and Runx2 transcriptional activity. J Biol Chem 279(36):37704–37715
33. Holland TA, Bodde EW, Cuijpers VM, Baggett LS, Tabata Y, Mikos AG, Jansen JA (2007) Degradable hydrogel scaffolds for in vivo delivery of single and dual growth factors in cartilage repair. Osteoarthr Cartil 15(2):187–197
34. Nagura I, Fujioka H, Kokubu T, Makino T, Sumi Y, Kurosaka M (2007) Repair of osteochondral defects with a new porous synthetic polymer scaffold. J Bone Joint Surg Br 89(2):258–264
35. Pei M, He F, Boyce BM, Kish VL (2009) Repair of full-thickness femoral condyle cartilage defects using allogeneic synovial cell-engineered tissue constructs. Osteoarthr Cartil 17(6):714–722
36. Huang X, Yang D, Yan W, Shi Z, Feng J, Gao Y, Weng W, Yan S (2007) Osteochondral repair using the combination of fibroblast growth factor and amorphous calcium phosphate/poly (L-lactic acid) hybrid materials. Biomaterials 28(20):3091–3100
37. van der Stok J, Koolen MK, de Maat MP, Yavari SA, Alblas J, Patka P, Verhaar JA, van Lieshout EM, Zadpoor AA, Weinans H, Jahr H (2015) Full regeneration of segmental bone defects using porous titanium implants loaded with BMP-2 containing fibrin gels. Eur Cell Mater 29(4):141–153
38. Niederauer GG, Slivka MA, Leatherbury NC, Korvick DL, Harroff HH, Ehler WC, Dunn CJ, Kieswetter K (2000) Evaluation of multiphase implants for repair of focal osteochondral defects in goats. Biomaterials 21(24):2561–2574
39. Lavery K, Hawley S, Swain P, Rooney R, Falb D, Alaoui-Ismaili MH (2009) New insights into BMP-7 mediated osteoblastic differentiation of primary human mesenchymal stem cells. Bone 45(1): 27–41
40. Bobyn JD, Toh KK, Hacking SA, Tanzer M, Krygier JJ (1999) Tissue response to porous tantalum acetabular cups: a canine model. J Arthroplasty 14(3):347–354
41. Duan X, Zhu X, Dong X, Yang J, Huang F, Cen S, Leung F, Fan H, Xiang Z (2013) Repair of large osteochondral defects in a beagle model with a novel type I collagen/glycosaminoglycan-porous titanium biphasic scaffold. Mater Sci Eng C Mater Biol Appl 33(7): 3951–3957
42. Jamil K, Chua KH, Joudi S, Ng SL, Yahaya NH (2015) Development of a cartilage composite utilizing porous tantalum, fibrin,and rabbit chondrocytes for treatment of cartilage defect. J Orthop Surg Res 10:27
43. Gordon WJ, Conzemius MG, Birdsall E, Wannemuehler Y, Mallapragada S, Lewallen DG, Yaszemski MJ, O'Driscoll SW (2005) Chondroconductive potential of tantalum trabecular metal. J Biomed Mater Res 75(2):229–233
44. Wang Q, Zhang H, Li Q, Ye L, Gan H, Liu Y, Wang H, Wang Z (2015) Biocompatibility and osteogenic properties of porous tantalum. Exp Ther Med 9(3):780–786
45. Depprich R, Zipprich H, Ommerborn M, Mahn E, Lammers L, Handschel J, Naujoks C, Wiesmann HP, Kübler NR, Meyer U (2008) Osseointegration of zirconia implants: an SEM observation of the bone-implant interface. Head Face Med 4(1):25